

NETWORK SCIENCE

Structure and dynamical behavior of non-normal networks

Malbor Asllani^{1,2}, Renaud Lambiotte¹, Timoteo Carletti^{2*}

We analyze a collection of empirical networks in a wide spectrum of disciplines and show that strong non-normality is ubiquitous in network science. Dynamical processes evolving on non-normal networks exhibit a peculiar behavior, as initial small disturbances may undergo a transient phase and be strongly amplified in linearly stable systems. In addition, eigenvalues may become extremely sensible to noise and have a diminished physical meaning. We identify structural properties of networks that are associated with non-normality and propose simple models to generate networks with a tunable level of non-normality. We also show the potential use of a variety of metrics capturing different aspects of non-normality and propose their potential use in the context of the stability of complex ecosystems.

INTRODUCTION

Network science (1–3) has emerged, in the past 20 years, as an essential framework to model and understand complex systems in a variety of disciplines, including physics (1), economics (4), biology (5), and sociology (6). At its core, network science views a system as a set of nodes that may be connected directly by an edge or indirectly by a succession of edges, thereby forming paths of interactions. The bridge between network structure and dynamics is generally unraveled by defining a linear dynamical model on the nodes; take, for instance, a random walk process as a simple model of diffusion or the linearization around a critical point of a nonlinear dynamical system (7–10). In each case, the process is determined by a matrix, somehow related to the adjacency matrix of the underlying network. In addition, critical aspects of the system, such as its stability and characteristic time scales, are usually described by the properties of its spectrum (11). Central network concepts such as the spectral gap, spectral radius, and master stability conditions all build on this interpretation. Relatedly, network spectra also appear in network algorithms, such as in community detection (12) or in network comparison (13).

The characterization of a linear system by its spectrum is canonical, but it is unreliable in situations when the linear operator is non-normal; namely, its eigenvectors do not necessarily form an orthonormal basis, and the transformation to eigenvector coordinates may involve a strong distortion of the phase space. Non-normality has a long tradition in linear algebra and dynamical systems, from early studies in hydrodynamics (14) to more recent works on the robustness of non-normal ecosystems (15) and in neuronal dynamics (16, 17). Yet, these results remain focused on limited areas of science, and a systematic study of the prevalence of non-normality in real-world networks, as well as its potential impact on dynamics, is still lacking. Here, we call non-normal a network whose adjacency matrix \mathbf{A} is non-normal (18). By definition, \mathbf{A} is non-normal if it verifies $\mathbf{A}\mathbf{A}^T \neq \mathbf{A}^T\mathbf{A}$. It is thus clear that \mathbf{A} needs to be asymmetric to be non-normal or, equivalently, the network needs to be directed to be non-normal, but, as we will discuss in more detail later, asymmetry is not sufficient and certain types of network architectures are necessary to determine a strong non-normality. Given a non-normal network, other standard matrices, such as its Laplacian \mathbf{L} , are also non-normal. Non-normality can hence be quantified using a standard spectral measure borrowed from matrix theory, such as Henrici's depar-

ture from normality (19), $d_F(\mathbf{M}) = \sqrt{\|\mathbf{M}\|_F^2 - \sum_{i=1}^n |\lambda_i|^2}$, where $\|\cdot\|_F$ is the Frobenius norm and λ_i are the eigenvalues of the adjacency matrix. A zero value is associated with a symmetric network, while the larger the values, the stronger the non-normality.

Before going further, let us briefly illustrate in more detail the influence of non-normality on the prototypical example of a linear (linearized) dynamics on a non-normal network. Without loss of generality, we consider the model $\dot{\mathbf{x}} = \mathbf{M}\mathbf{x}$, where \mathbf{M} encodes the linear dynamics on the network, through the dependence on \mathbf{L} , and forms a stable matrix; namely, the spectral abscissa $\alpha(\mathbf{M}) = \max \Re \sigma(\mathbf{M})$ is not positive, with $\sigma(\mathbf{M})$ being the spectrum of the matrix \mathbf{M} . In the case of normal networks, the solution of the linear system would consist of a linear combination of exponentially relaxing modes, each with a characteristic time scale given by the inverse of the corresponding eigenvalue; hence, the spectral abscissa is responsible for the long-term dynamics. In situations when the network is non-normal, however, more complex patterns may emerge. Standard measures of non-normality of the matrix and their relation to dynamics are provided in Table 1. If \mathbf{M} has a positive numerical abscissa, $\omega(\mathbf{M}) = \max \sigma(H(\mathbf{M}))$, where $H(\mathbf{M}) = (\mathbf{M} + \mathbf{M}^T)/2$ is the Hermitian part of \mathbf{M} , then the system can undergo a transient growth before asymptotically converging to zero, as measured by the norm of the state vector \mathbf{x} (see Table 1A). This transient behavior cannot be explained by the picture provided by the spectrum of the matrix \mathbf{M} (19) and can have a strong impact once nonlinearities are at play. In situations when the dynamics is obtained from the linearization around a critical point, this initial growth may trigger nonlinear terms, take the system far away from the equilibrium, and thus radically reshape the dynamical behavior of nonlinear systems (18), as shown in Table 1B.

Although a system can initially be close to an asymptotically stable equilibrium, it can leave this state even when a moderate external perturbation occurs due to non-normality (19). This effect is even more notable once one includes stochastic forces to the model, e.g., exogenous or demographic perturbations due to the surrounding environment (20), as they may push even a linear, stable system out of equilibrium when it is non-normal. Again, this behavior cannot be properly captured by the spectrum of the linear model, nor can it be described by the numerical abscissa, which only determines the short-term behavior of the dynamics. To describe the long-term consequences of these perturbations, another important tool is the pseudospectrum $\sigma_\epsilon(\mathbf{M}) = \{\sigma(\mathbf{M} + \mathbf{E}) : \|\mathbf{E}\| \leq \epsilon\}$, for $\epsilon > 0$ (19), from which one can compute the ϵ -pseudospectral abscissa, replacing somehow the role of the spectral abscissa and eventually the Kreiss constant \mathcal{K} , which provides a direct measure of the size of the transient amplification (see Table 1). By

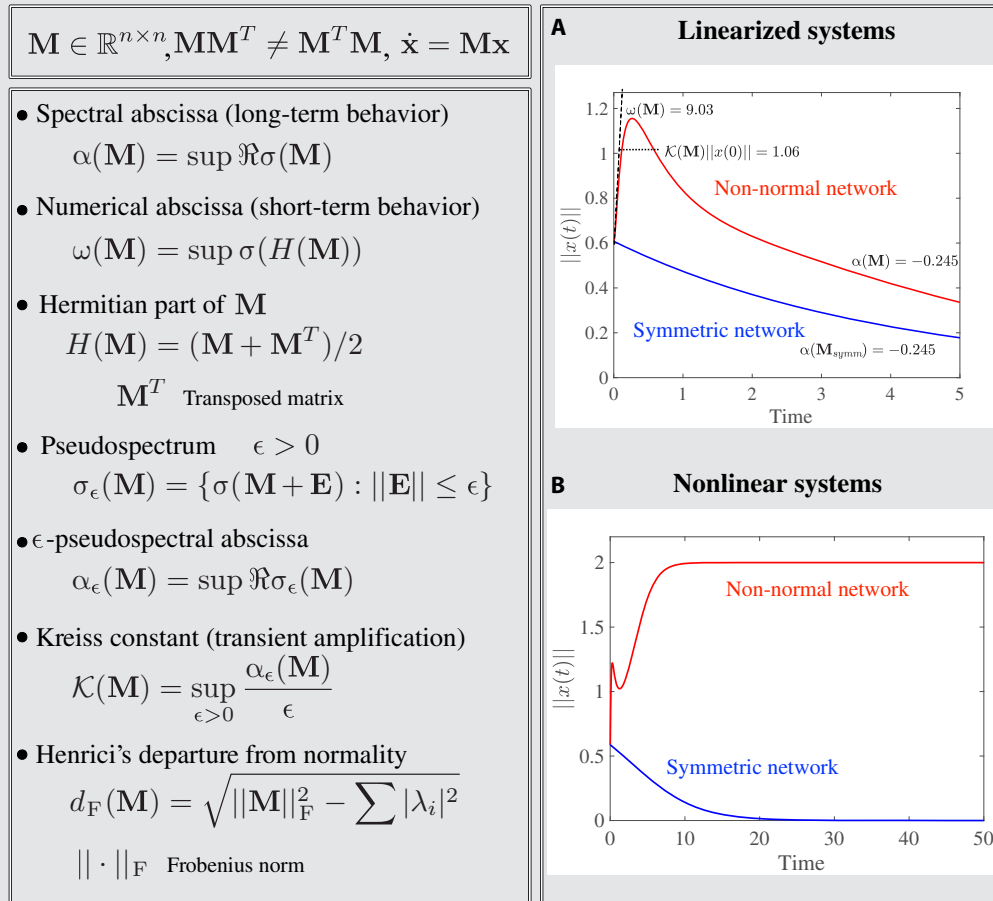
Copyright © 2018
The Authors, some
rights reserved;
exclusive licensee
American Association
for the Advancement
of Science. No claim to
original U.S. Government
Works. Distributed
under a Creative
Commons Attribution
NonCommercial
License 4.0 (CC BY-NC).

¹Mathematical Institute, University of Oxford, Woodstock Rd, OX2 6GG Oxford, UK.

²Department of Mathematics and naXys, Namur Institute for Complex Systems, University of Namur, rempart de la Vierge 8, B 5000 Namur, Belgium.

*Corresponding author. Email: timoteo.carletti@unamur.be

Table 1. Summary of non-normal dynamics. In the left panel, we summarize some of the main concepts related to non-normal dynamics. They are illustrated through the time evolution of the norm of the solution of the nonlinear bistable system $\dot{x}_i = f(x_i) + D(\mathbf{L}\mathbf{x})_i$, where $f(x) = x(a - x)(x - 1)$ [(B) on the right] and its linearization, $\dot{\mathbf{x}} = \mathbf{M}\mathbf{x}$, around the stable equilibrium $\mathbf{x} = 0$ [(A) on the right]. Here, $\mathbf{M} = a\mathbf{I} + D\mathbf{L}$, $a = -0.245$, $D = 10$, \mathbf{I} is the identity matrix, and \mathbf{L} is the Laplacian matrix of the underlying non-normal network (3). Observe that the system is asymptotically stable, $\alpha(\mathbf{M}) = a < 0$. On both panels on the right, the red curves correspond to a non-normal scale-free (nSF) network, while the blue ones correspond to the symmetric version of the same network. Both systems are asymptotically stable and their solutions decrease to asymptotically reach the stable point (A) $\mathbf{x} = 0$. However, one can appreciate the nonmonotone convergence of the red curve due to an initial growth induced by a positive $\omega(\mathbf{M})$ and estimated by the Kreiss constant. This different behavior has a notable consequence in the nonlinear model (B). In that case, even if the equilibrium point remains stable, the initial amplification due to non-normality is sufficiently strong to push the orbit toward another equilibrium identified by an asymptotic positive amplitude $\|x(t)\| > 0$ for $t \rightarrow \infty$.



definition, a complex number z is an eigenvalue of \mathbf{M} if a bounded inverse of $z\mathbf{I} - \mathbf{M}$ does not exist. The pseudospectrum is based on a less strict definition and defines regions of the complex plane where $\|(z\mathbf{I} - \mathbf{M})^{-1}\|$ is larger than a prescribed positive number ϵ^{-1} . By its very first definition, the pseudospectrum defines regions of the complex plane where eigenvalues of a matrix can be found because of a small perturbation, $\mathbf{M} + \Delta\mathbf{M}$, with $\|\Delta\mathbf{M}\| < \epsilon$. These perturbations lead to small variations of the spectrum in the case of normal matrices, but they can become much more important in the case of non-normal matrices. In particular, even small perturbations can make a linearly stable system unstable. Note that this effect may have important practical consequences for networks, as the precise value of edge weights is often unknown (21), and empirical measurements of networks are prone to missing edges (22).

As we have discussed, non-normality may strongly affect linear and nonlinear dynamical systems on networks and, more generally, their behavior. The contributions of this work are manifold. First, we show

that a strong non-normality is widespread in complex networks empirically observed in a variety of domains. As a second step, we reveal the organization behind non-normality and show that non-normality is associated with a combination of absence of cycles (23), low reciprocity (24), and hierarchical organization (25). We also propose a simple model for growing networks based on preferential attachment reproducing our observations. Last, we consider in detail a Lotka-Volterra model applied to a real-world network and show that the use of network metrics for non-normality helps to understand the dynamics of the system.

RESULTS

Non-normal networks: Empirical data and the shape of non-normality

As a first step, we have considered a large set of directed, real-world networks from different disciplines, including biology, sociology,

communication, transport, and many more. Results reported in Table 2 (see also the more complete table presented in the Supplementary Materials) show values of standard measures of non-normality, including the numerical abscissa, the ϵ -pseudospectral abscissa, and the normalized Henrici's departure from normality, $\hat{d}_F(\mathbf{M}) = d_F(\mathbf{M})/\|\mathbf{M}\|_F$, all revealing that the networks present a strong non-normality.

As a next step, we investigate the type of network organization associated with non-normality. The directedness and low reciprocity of a network are necessary conditions for non-normality, but they are by no means sufficient. For instance, a k -regular directed ring, whose adjacency matrix is circulant, is normal because of its rotational symmetry (18). The condition $\mathbf{A}\mathbf{A}^T \neq \mathbf{A}^T\mathbf{A}$ is instead satisfied when the network is

hierarchical, that is, when nodes have a rank and edges with a strong weight tend to flow from nodes with a small rank to nodes with a high rank (or vice versa). These organizations are known to be prevalent in different types of networks (25–28), for instance, through the concepts of dominance hierarchies in social ecology, trophic levels in food webs, and social status in social networks. The inequality becomes maximum when the network is a directed acyclic graph (DAG), such that the matrix takes an upper triangular form after proper relabeling of the nodes. Again, DAGs find several applications, for instance, in the case of citation or causal networks. On the basis of these intuitions, we estimate the level of hierarchy of a real-world network as follows. Given an adjacency matrix, we search for the best nodes ordering such that the

Table 2. Some figures for a selected set of real webs. We report values of metrics associated with non-normality for a selection of well-studied real-world networks, whose numbers of nodes and links span several orders of magnitude. A more complete table is available in the Supplementary Materials. All networks are weighted and directed and appear to have a pronounced non-normality. Their adjacency matrix \mathbf{A} satisfies $\mathbf{A}\mathbf{A}^T \neq \mathbf{A}^T\mathbf{A}$, and they have a positive numerical abscissa (ω)—i.e., they are reactive—which is much larger than the corresponding spectral abscissa (α); almost all the values in the column $\omega - \alpha$ are strongly positive. Moreover, the ϵ -pseudospectral abscissa, α_ϵ (see Table 1), is positive for the value $\epsilon = 10^{-1/2}$. The normalized Henrici's departure from normality, \hat{d}_F (see Table 1 and Methods), is also often very large. We observe that, in the case of very large networks, denoted with an asterisk (*), we have only been able to provide an upper bound for this index, by computing the 1000 largest eigenvalues. We also report the structural measure of asymmetry Δ , which is correlated with \hat{d}_F (see text and Fig. 1B). Additional details are provided in figs. S4 and S5.

Network name	Nodes	Links	ω	$\omega - \alpha$	α_ϵ	Δ	\hat{d}_F
Foodwebs							
Cypress wetlands South Florida (wet)	128	2016	296.71	132.11	167.46	0.83	1.00
Cypress wetlands South Florida (dry)	128	2137	217.60	152.50	82.20	0.89	1.00
Little Rock Lake (Wisconsin, USA)	183	2494	21.69	14.69	10.02	0.95	0.93
Biological							
Transcriptional regulation network (<i>Escherichia coli</i>)	423	578	5.11	4.11	2.52	0.81	0.93
Metabolic network (<i>Caenorhabditis elegans</i>)	453	4596	13.44	12.44	6.89	0.98	1.00
Pairwise proteins interaction (<i>Homo sapiens</i>)	2239	6452	15.79	13.02	4.01	0.99	0.99
Transport							
U.S. airport 2010	1574	28,236	1.19×10^7	79.30	1.19×10^7	0.01	1.00
Road transportation network (Rome)	3353	8870	2.40×10^4	120.05	2.39×10^4	0.08	0.28
Road transportation network (Chicago)	12,982	39,018	4.23	4.29×10^{-4}	4.54	0.04	0.19
Communication							
Email network Democratic National Committee	2029	39,264	28.00	2.00	26.37	0.53	0.89
Enron email network (1999–2003)	87,273	1,148,072	85.14	14.54	71.05	0.30	0.99*
Email network European institution	265,214	420,045	76.02	6.09	70.30	0.30	0.84*
Citation							
Citations to Milgram's 1967 paper (2002)	395	1988	10.48	10.48	4.49	1.00	1.00
Articles from <i>Scientometrics</i> (1978–2000)	3084	10,416	10.32	8.32	5.28	0.98	1.00
Citation network Digital Bibliography and Library Project	12,591	49,743	21.50	16.82	8.45	0.87	1.00
Social							
Hypertext network of 2004 U.S. election blogs	1224	19,025	45.37	10.95	34.95	0.72	0.98
Reply network of the news website Digg	30,398	87,627	15.92	6.56	10.18	0.61	0.97
Trust network from the website Epinions	75,879	508,837	123.00	16.47	106.96	0.13	0.80*

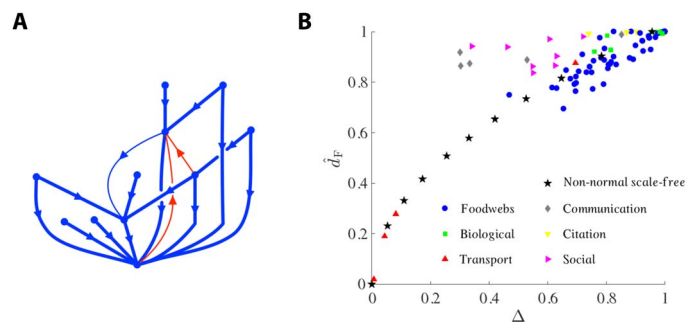


Fig. 1. Structure of non-normal networks. (A) DAG (blue links) embedded in a weighted non-normal network, with red links corresponding to entries in the lower triangular part of the adjacency matrix (once nodes are reordered). The thickness of a link is proportional to its weight. (B) Normalized Henrici's departure from normality versus the structural measure of asymmetry Δ , for the networks of table S1 and for the nSF model.

total weight in the upper triangular part of the matrix is maximal (see Methods), thus allowing one to identify the DAG of maximum weight embedded in the network. A simple measure of asymmetry is then the unbalance Δ between the number of entries in the upper and lower triangular part of the relabeled adjacency matrix $\tilde{\mathbf{A}}$, that is, $\Delta := |K^< - K^>|/K$, where $K^< = \sum_i \sum_j \tilde{A}_{ij}$, $K^> = \sum_i \sum_j \tilde{A}_{ji}$, and $K = K^< + K^>$. Δ thus measures the asymmetry of the adjacency matrix after relabeling, and it provides a structural indicator of non-normality that can be compared with standard spectral measures, such as the normalized Henrici's departure from normality. In Fig. 1B, we show that the normalized Henrici's index strongly correlates with Δ across a variety of real-world networks, hence reinforcing the connection between structural hierarchy and dynamical non-normality (see also Methods). Last, note that non-normality and a hierarchical structure are global properties of a network. As an illustration, we have considered in the Supplementary Materials the case of networks built from different combinations of the same constituting blocks or motifs (25, 29–31), and we observe that different levels of non-normality can emerge from the combination of two directed motifs, from strong non-normality and a DAG structure for the whole graph to weakly non-normal patterns, where the presence of a cycle prevents the dynamical flow to accumulate on a small number of nodes.

Mechanistic model

Here, we propose a simple mechanistic model, denoted by the nSF network, leading to the formation of networks with tunable levels of non-normality. The model builds on the seminal ideas of de Solla Price (32), later leading to the family of preferential attachment models (33). As discussed before, critical ingredients of the model should be the low reciprocity of the directed edges and the presence of a hierarchical structure. We thus consider a growing network where, at each step, a new node j draws a directed edge to a previously existing node i , with a probability proportional to its in-degree. Note that this type of process is expected to lead to the formation of power-law in-degree distributions, but this is not our concern here. Node i also has the possibility of reciprocating and creating a link directed at j , as in (34). Asymmetry can be included in different ways, either by endowing edges with a weight and imposing that $0 \leq w_{ji} \ll w_{ij}$ or by considering unweighted edges and assuming that the reciprocal edge is created with a probability $p_{i \rightarrow j} \ll 1$, see Fig. 2. Hierarchy is then induced by the ordering of the nodes in terms of their arrival time. As expected, the stronger the inequalities,

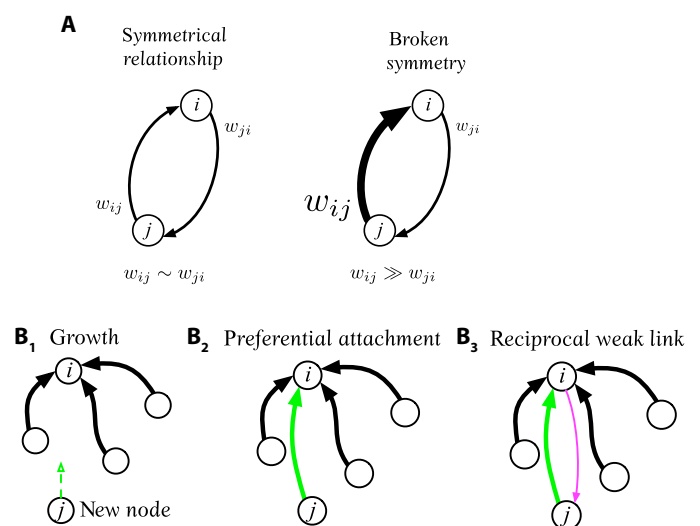


Fig. 2. nSF network. (A) Local breaking of reciprocity: If j 's influence over i is larger than the reciprocal one, the pairwise relation is nonreciprocal and presents a broken symmetry. (B) Generating model of nSF network: Once a new node enters the system (dashed green arrow in B₁), it establishes, with higher probability, a link pointing toward the node with larger in-degree, i (solid green link in B₂). With a lower probability, the latter, i.e., the hub, can create a weaker link pointing to the reciprocal direction (thin magenta link in B₃).

the stronger the non-normality of the resulting networks. We have investigated the non-normality of the resulting networks and found a notable similarity with the relation between Δ and Henrici's departure from normality observed in real-world networks, as shown in Fig. 1. Note that we have also considered variants of other classical network models, such as Erdős-Rényi (ER) (35) and Watts-Strogatz (WS) (36) (see the Supplementary Materials), but their lack of hierarchical structure prevents the formation of strong non-normality, as can be seen in their pseudospectral properties (see Fig. 3 and the Supplementary Materials).

Application to the stability of complex ecosystems

The hierarchical structure of non-normal networks allows for the introduction of interesting connections with dynamical systems. Here, we focus on stability, a central concept to understand the emergence of collective phenomena (10). The importance of network structure for stability is well established since the seminal works of May (7) and Allesina and Tang (8) in the context of ecology. For instance, choosing the interaction strengths from a normal distribution $\mathcal{N}(0, \sigma)$, May proved that an ecosystem loses its stability above a critical size, as a consequence of the circular law (37). To understand the interplay of non-normality and dynamics, we analyze the master stability function (3, 10), which is a general tool that allows one to infer about the (in)stability of a networked dynamical system; it often relies on the use of the spectrum of some suitable linearization, while hereby conditions for (in)stability are determined through the pseudospectrum of the linearized system (1). The latter represents the generalized Lotka-Volterra (GLV) model, which is popular for understanding competition and mutualism among interacting species (7–9). The set of equations governing the dynamics of trophic interactions is given by (9)

$$\frac{dx_i}{dt} = x_i \left(r_i - s_i x_i + \sum_{j \neq i} M_{ij} x_j \right), \forall i = 1, 2, \dots, N \quad (1)$$

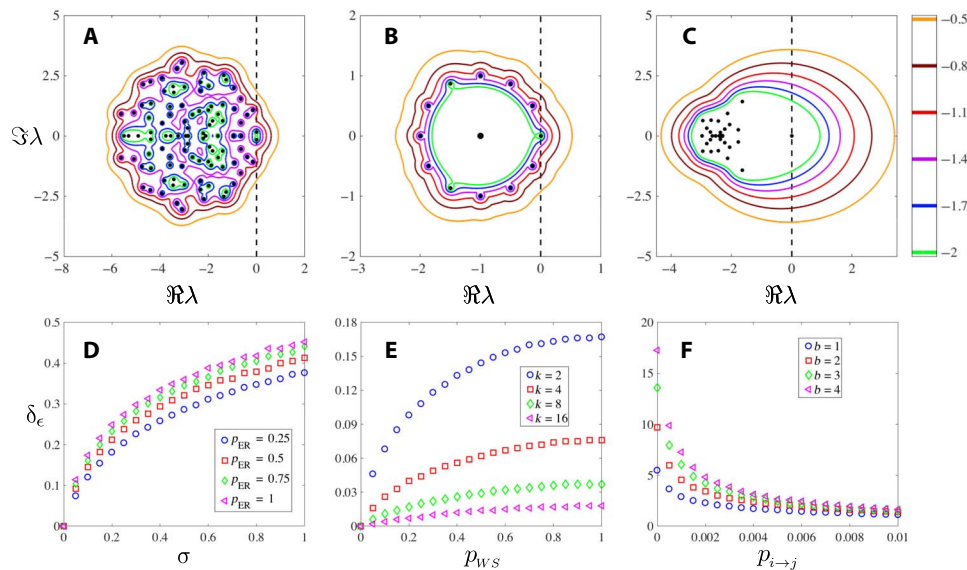


Fig. 3. Models of non-normal networks. Spectra and pseudospectra [computed using the software EigTool (44)] of non-normal models (top): (A) ER with link probability $p_{ER} = 0.1$ and weights from a normal distribution $\mathcal{N}(0, 1)$, (B) (unweighted) WS with initial number of neighbor nodes $k = 2$ and rewiring probability $p_{WS} = 1$, (C) nSF network with probability of backward links $p_{i \rightarrow j} = 0.001$ for $j > i$ and weights from a uniform distribution, $\mathcal{U}[0, 1]$. The color bar on the right represents the different levels of $\|E\|$ in log scale, e.g., $\epsilon = 10^x$, where x is the numerical value reported on the bar. Visual inspection reveals that the pseudospectrum of diverse network models is affected differently by ϵ and, in particular, that its size is increased more substantially for the nSF model. In the bottom panels, we quantify how the size increase of the pseudospectrum affects the stability of its network as follows. We consider the difference between the ϵ -pseudoabscissa of A and that of its Hermitian part, $\delta_\epsilon = \alpha_\epsilon(\mathbf{A}) - \alpha_\epsilon(H(\mathbf{A}))$, hence measuring how the non-Hermitian aspect of the system affects its dominant eigenvalue. This quantity is always positive, as the pseudospectrum of a non-normal matrix is larger than that of a normal one (19), for any given fixed $\epsilon > 0$. (D) ER with weights from a normal distribution $\mathcal{N}(0, \sigma)$ for several values of the variance and different link probabilities, p_{ER} . (E) (Unweighted) WS for different rewiring probabilities p_{WS} and different initial number of neighbor nodes k . (F) nSF with varying backward link probability $p_{i \rightarrow j}$ and different upper bound, b , of the uniform distribution from which the weights are chosen, $\mathcal{U}[0, b]$. In each case, the networks are composed of 100 nodes, and the adjacency matrices have been diagonally shifted with their respective spectral abscissa $\alpha(\mathbf{A})$, to set the real part of the maximum of each spectrum exactly at 0. For the bottom panels, the value of ϵ has been set to $10^{-0.5}$.

Here, r_i are the intrinsic rates of (i) birth if $r_i > 0$, meaning that species i can reproduce itself in absence of other species and in abundance of resources; (ii) death if $r_i < 0$ in the sense that the population of species i will decline in absence of other species (e.g., preys). The positive constants s_i represent the finite carrying capacity of the ecosystem (limited resources) and prevent the species i from growing indefinitely. An important role is played by the community matrix \mathbf{M} , whose entries M_{ij} (respectively M_{ji}) represent the influence of species j on i (respectively i on j). We also assume that $M_{ii} = 0$, $\forall i$; namely, the community matrix describes only interspecies interactions, and intraspecies interactions have been cast into s_i . In the following, we adopt the method of Chen and Cohen (38), as already explained in the literature (8, 9). More precisely, we hypothesize the existence of a positive equilibrium solution \mathbf{x}^* that, without loss of generality, can be assumed to be of the form $x_i^* = 1$, for all i , after a suitable choice of the growth/death rates r_i . At this point, the master stability function of the GLV model depends solely on the spectrum (pseudospectrum) of the matrix $\mathbf{M} - \text{diag}(s)$, namely, the community matrix from which we remove the matrix whose diagonal contains the interspecies strengths s_i . The problem is hence mapped to a framework where stability directly depends on species interactions.

The vulnerability of the system is visible in Fig. 4, where the spectra (black dots) shift from the left to the right of the imaginary axis once mutualism increases. Although the system remains stable for a strong competitive setting (Fig. 4, A and B), we can observe (colored curves) that the ϵ -pseudospectral abscissa [see (19) and Table 1] is positive and larger for structured systems than for random

ones (8). To represent the former systems, we used the nSF networks obtained with the generation model previously presented, the latter exhibiting features very similar to the real trophic relations. This implies that the system can easily be destabilized by (relatively) small fluctuations due to demographic, thermal, or endogenous noise that are always present in the surrounding environment and are amplified because of the non-normality (see the Supplementary Materials). This remark can have important consequences in the understanding of the problem of coexistence of multiple species in a harsh competitive environment, e.g., in the case of the paradox of the plankton (39), for which field observations are at odds with the principle of competitive exclusion (8).

DISCUSSION AND CONCLUSIONS

We have shown that a large number of real-life networks are strongly non-normal and that a characterization of their properties solely by spectral methods may be misleading. Non-normality induces a strong dependency on fluctuations and needs to be considered with care when performing a linear stability analysis of nonlinear systems. Despite the fact that the non-normality is well studied and that its importance has been recognized in a variety of domains, a systematic analysis of its importance and effect in large-scale networks was still lacking. Our first contribution is thus not only the identification of what appears to be a ubiquitous property of directed networks but also the introduction of new methods in the toolbox of network science to generate non-normal networks and capture the effect of non-normality on their dynamics. Potential applications have recently been explored, for instance,

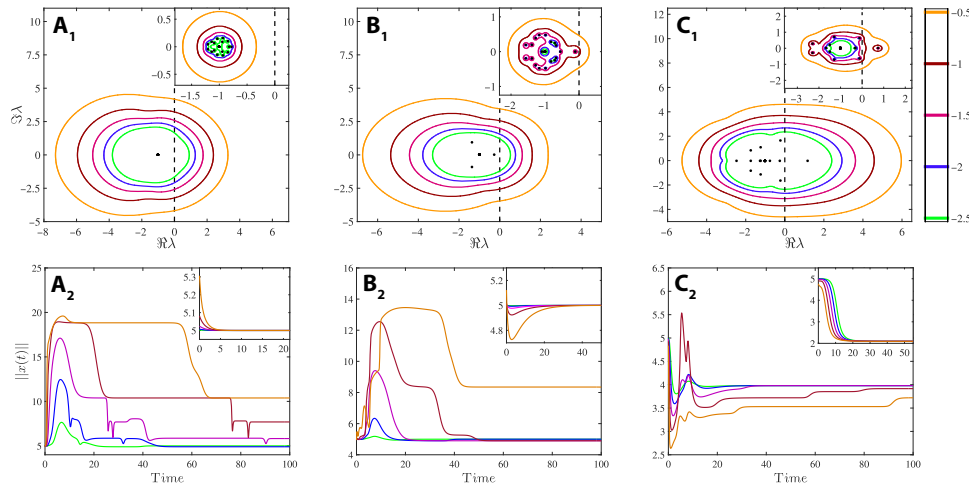


Fig. 4. GLV model: $\dot{\mathbf{x}}_i = \mathbf{x}_i(\mathbf{r}_i - \mathbf{s}_i\mathbf{x}_i + \sum_{j \neq i} \mathbf{M}_{ij}\mathbf{x}_j)$. We consider an ecosystem composed of 25 species. For the sake of simplicity, the intraspecies interactions are all set equal, $s_i = 1 \ \forall i$, and \mathbf{M} is the (weighted and signed) adjacency matrix of an nSF for the structured case (main panels) or a random matrix (insets) whose weights are drawn from a normal distribution $\mathcal{N}(0, 1/5)$. In the structured cases, the strengths in the upper triangular part of the matrix \mathbf{M} are 15 times larger than those in the lower one, thus enhancing non-normality, as can be seen from the pseudospectrum levels [computed using the software EigTool (44)]. In the top panels, we show the master stability function close to the asymptotically stable equilibrium point, based on the use of the pseudospectra. The corresponding dynamical evolution is shown in the bottom panels, where different colors correspond to different levels of ϵ in log scale (as in the top panels); initial conditions have been uniformly randomly chosen. Different cases are considered depending on the signs of the interaction strengths: **(A)** competition ($-/-$), **(B)** prey-predator ($-/+$), and **(C)** mutualism ($+/+$). We observe that, even if the system is asymptotically stable (A_1 and B_1), the ϵ -pseudospectral abscissa is positive for sufficiently large ϵ , thus inducing an unstable system behavior if the perturbation (in the adjacency matrix and/or in the initial conditions) is strong enough (A_2 and B_2). Yet, the unstructured systems still converge to the homogeneous equilibrium [see insets in (A_2) and (B_2)]. Overall, this effect is more pronounced in the structured systems than in the random ones, as the ϵ levels are much larger in the former case, for a fixed value of ϵ .

in pattern formation on networks (18) and in epidemic spreading in metapopulation models (18). Overall, these findings emphasize that non-normality is a critical component of complex systems and that specific tools are necessary to complement standard methods based on eigenspectra, which are prevalent in network science. More specifically, this new perspective may shed light on how to explain the diversity of species in ecosystems (40), the origin of cascade failures in power grids (41), or the spread of epidemics in mobility networks (42), just to mention a few possible applications.

METHODS

Measures of non-normality

A real matrix \mathbf{M} is said to be non-normal if it is not diagonalizable by a unitary matrix; namely, its eigenvectors are not orthogonal to each other (19). The numerical abscissa has been introduced in population dynamics (15) with the term of reactivity, and it is defined by $\omega(\mathbf{M}) = \sup \sigma(H(\mathbf{M}))$, where $H(\mathbf{M}) = (\mathbf{M} + \mathbf{M}^T)/2$ is the Hermitian part of \mathbf{M} . This is a very natural concept; however, it does not allow the computation of the maximum amplification of the initial conditions exhibited by linear stable non-normal systems. For this reason, one has to resort to the pseudospectrum (19), $\sigma_\epsilon(\mathbf{M})$, which is defined for all $\epsilon > 0$ as the spectrum of the perturbed matrix $\mathbf{M} + \mathbf{E}$, for any matrix $\|\mathbf{E}\| \leq \epsilon$. From the ϵ -pseudospectral abscissa, $\alpha_\epsilon(\mathbf{M}) = \sup \Re \sigma_\epsilon(\mathbf{M})$, we can obtain the Kreiss constant, $\mathcal{K}(\mathbf{M}) = \sup_{\epsilon > 0} \alpha_\epsilon(\mathbf{M})/\epsilon$, and eventually the lower bound on the orbit size

$$\sup_{t \geq 0} \|\mathbf{x}(t)\| \geq \mathcal{K}(\mathbf{M}) \|\mathbf{x}(0)\| \quad (2)$$

Let us observe that the latter provides a straightforward bound on the amplification envelope defined in (15). Moreover, $\mathcal{K}(\mathbf{M})$ is more informative than reactivity, in fact a stable system, can exhibit a small amplification even if $\omega(\mathbf{M}) > 0$ is very large.

Henrici's index is based on the observation that the Frobenius norm of a normal matrix is given by $\|\mathbf{M}\|_F^2 = \text{tr}(\mathbf{M}^T \mathbf{M}) = \sum_{i=1}^n |\lambda_i|^2$, where λ_i are the eigenvalues of the matrix; one can thus define Henrici's departure from normality (19) for a non-normal matrix \mathbf{M} by

$$d_F(\mathbf{M}) = \sqrt{\|\mathbf{M}\|_F^2 - \sum_{i=1}^n |\lambda_i|^2} \quad (3)$$

It attains its minimum once the matrix is normal and then increases as long as the matrix deviates from normality. To compare systems with different sizes, we define the normalized index $\hat{d}_F(\mathbf{M}) = d_F(\mathbf{M})/\|\mathbf{M}\|_F$.

For a generic matrix with binary (respectively positive) entries, one can define the imbalance between the number (respectively the total sum) of entries in the upper and lower triangular part, using the language of networks

$$\Delta(\mathbf{M}) := \frac{\left| \left(\sum_{i < j} \tilde{M}_{ij} - \sum_{j < i} \tilde{M}_{ij} \right) \right|}{\left(\sum_{i < j} \tilde{M}_{ij} + \sum_{j < i} \tilde{M}_{ij} \right)} \quad (4)$$

where \tilde{M}_{ij} are the entries of the final relabeled matrix.

While it can be relatively easy to determine a DAG and compute Δ , once we have a drawing of a (small enough) network, this task becomes hard starting from the adjacency matrix or a large network. We observed that the simple operation of relabeling the nodes can change the value of Δ and that the latter increases the larger the number of entries in the adjacency matrix in the upper triangular part, namely, links $i \rightarrow j$, where $j > i$. Having in mind these observations, we designed an algorithm aiming at maximizing Δ once couples of nodes are relabeled; i.e., rows and columns of the adjacency matrix are swapped. To overcome the combinatorial difficulty of the problem, we resorted to a simulated annealing method (43) to get an accurate solution in a relatively short time. A pseudocode is presented in the Supplementary Materials, and the generic convergence behavior of the maximization process is shown in fig. S2.

SUPPLEMENTARY MATERIALS

Supplementary material for this article is available at <http://advances.sciencemag.org/cgi/content/full/4/12/eaau9403/DC1>

Section S1. Non-normal matrices and their pseudospectra

Section S2. Global structure of non-normal networks

Section S3. Models for generation of non-normal networks

Section S4. An intuitive meaning of the pseudospectrum

Section S5. Pseudospectra of real non-normal networks

Section S6. Extended table of real non-normal networks

Fig. S1. Time evolution of the norm of the solution of the linear ordinary differential equation $\dot{\mathbf{x}} = \mathbf{M}\mathbf{x}$.

Fig. S2. Convergence of the maximization algorithm.

Fig. S3. Henrici's departure from normality versus Δ .

Fig. S4. Motifs organization and non-normality.

Fig. S5. Spectra and pseudospectra of non-normal networks.

Fig. S6. Pseudospectra for real networks I.

Fig. S7. Pseudospectra for real networks II.

Table S1. Some figures for real webs.

References (45–80)

REFERENCES AND NOTES

1. R. Albert, A.-L. Barabási, Statistical mechanics of complex networks. *Rev. Mod. Phys.* **74**, 47–97 (2002).
2. S. Boccaletti, V. Latora, Y. Moreno, M. Chavez, D.-U. Hwang, Complex networks: Structure and dynamics. *Phys. Rep.* **424**, 175–308 (2006).
3. M. E. J. Newman, *Networks: An Introduction* (Oxford Univ. Press, 2010).
4. M. O. Jackson, *Social and Economic Networks* (Princeton Univ. Press, 2008).
5. A.-L. Barabási, N. Gulbahce, J. Loscalzo, Network medicine: A network-based approach to human disease. *Nat. Rev. Genet.* **12**, 56–68 (2011).
6. S. Wasserman, K. Faust, *Social Network Analysis: Methods and Applications* (Cambridge Univ. Press, ed. 1, 1994).
7. R. M. May, Will a large complex system be stable? *Nature* **238**, 413–414 (1972).
8. S. Allesina, S. Tang, Stability criteria for complex ecosystems. *Nature* **483**, 205–208 (2012).
9. K. Z. Coyte, J. Schuler, K. R. Foster, The ecology of the microbiome: Networks, competition, and stability. *Science* **350**, 663–666 (2015).
10. L. M. Pecora, T. L. Carroll, Master stability functions for synchronized coupled systems. *Phys. Rev. Lett.* **80**, 2109–2112 (1998).
11. P. Van Mieghem, *Graph Spectra for Complex Networks* (Cambridge Univ. Press, 2010).
12. M. E. J. Newman, Finding community structure in networks using the eigenvectors of matrices. *Phys. Rev. E* **74**, 036104 (2006).
13. C. Donnat, S. Holmes, Tracking network dynamics: A survey of distances and similarity metrics. *arXiv:1801.07351 [stat.AP]* (9 March 2018).
14. L. N. Trefethen, A. E. Trefethen, S. C. Reddy, T. A. Driscoll, Hydrodynamic stability without eigenvalues. *Science* **261**, 578–584 (1993).
15. M. G. Neubert, H. Caswell, Alternatives to resilience for measuring the responses of ecological systems to perturbations. *Ecology* **78**, 653–665 (1997).
16. B. K. Murphy, K. D. Miller, Balanced amplification: A new mechanism of selective amplification of neural activity patterns. *Neuron* **61**, 635–648 (2009).
17. G. Hennequin, T. P. Vogels, W. Gerstner, Non-normal amplification in random balanced neuronal networks. *Phys. Rev. E* **86**, 011909 (2012).
18. M. Asllani, T. Carletti, Topological resilience in non-normal networked systems. *Phys. Rev. E* **97**, 042302 (2018).
19. L. N. Trefethen, M. Embree, *Spectra and Pseudospectra: The Behavior of Nonnormal Matrices and Operators* (Princeton Univ. Press, 2005).
20. C. W. Gardiner, *Handbook of Stochastic Methods: For Physics, Chemistry and the Natural Sciences* (Springer, ed. 3, 2004).
21. Y.-Y. Liu, J.-J. Slotine, A.-L. Barabási, Controllability of complex networks. *Nature* **473**, 167–173 (2011).
22. D. Liben-Nowell, J. Kleinberg, The link-prediction problem for social networks. *J. Am. Soc. Inf. Sci. Technol.* **58**, 1019–1031 (2007).
23. S. Johnson, N. S. Jones, Looplessness in networks is linked to trophic coherence. *Proc. Natl. Acad. Sci. U.S.A.* **114**, 5618–5623 (2017).
24. T. Squartini, F. Picciolo, F. Ruzzenenti, D. Garlaschelli, Reciprocity of weighted networks. *Sci. Rep.* **3**, 2729 (2013).
25. B. Corominas-Murtra, J. Goñi, R. V. Solé, C. Rodríguez-Caso, On the origins of hierarchy in complex networks. *Proc. Natl. Acad. Sci. U.S.A.* **110**, 13316–13321 (2013).
26. E. Ravasz, A.-L. Barabási, Hierarchical organization in complex networks. *Phys. Rev. E* **67**, 026112 (2003).
27. D. Czégel, G. Palla, Random walk hierarchy measure: What is more hierarchical, a chain, a tree or a star? *Sci. Rep.* **5**, 17994 (2015).
28. C. De Bacco, D. B. Larremore, C. Moore, A physical model for efficient ranking in networks. *Sci. Adv.* **4**, eaar8260 (2018).
29. R. Milo, S. Shen-Orr, S. Itzkovitz, N. Kashtan, D. Chklovskii, U. Alon, Network motifs: Simple building blocks of complex networks. *Science* **298**, 824–827 (2002).
30. R. Milo, S. Itzkovitz, N. Kashtan, R. Levitt, S. Shen-Orr, I. Ayzenshtat, M. Sheffer, U. Alon, Superfamilies of evolved and designed networks. *Science* **303**, 1538–1542 (2004).
31. T. E. Gorochowski, C. S. Grierson, M. di Bernardo, Organization of feed-forward loop motifs reveals architectural principles in natural and engineered networks. *Sci. Adv.* **4**, eaap9751 (2018).
32. D. J. de Solla Price, Networks of scientific papers. *Science* **149**, 510–515 (1965).
33. A. Barabási, R. Albert, Emergence of scaling in random networks. *Science* **286**, 509–512 (1999).
34. V. Zlatić, H. Štefanić, Model of Wikipedia growth based on information exchange via reciprocal arcs. *Europhys. Lett.* **93**, 58005 (2011).
35. P. Erdős, A. Rényi, On the evolution of random graphs. *Publ. Math. Inst. Hung. Acad. Sci.* **5**, 17–61 (1960).
36. D. J. Watts, S. H. Strogatz, Collective dynamics of ‘small-world’ networks. *Nature* **393**, 440–442 (1998).
37. T. Tao, V. H. Vu, Random matrices: The circular law. *Commun. Contemp. Math.* **10**, 261–307 (2008).
38. X. Chen, J. E. Cohen, Global stability, local stability and permanence in model food webs. *J. Theor. Biol.* **212**, 223–235 (2001).
39. G. E. Hutchinson, The paradox of the plankton. *Am. Nat.* **95**, 137–145 (1961).
40. P. Chesson, Mechanisms of maintenance of species diversity. *Annu. Rev. Ecol. Syst.* **31**, 343–366 (2000).
41. S. V. Buldyrev, R. Parshani, G. Paul, H. E. Stanley, S. Havlin, Catastrophic cascade of failures in interdependent networks. *Nature* **464**, 1025–1028 (2010).
42. V. Colizza, A. Barrat, M. Barthélemy, A. Vespignani, The role of the airline transportation network in the prediction and predictability of global epidemics. *Proc. Natl. Acad. Sci. U.S.A.* **103**, 2015–2020 (2006).
43. P. J. M. van Laarhoven, E. H. L. Aarts, *Simulated Annealing: Theory and Applications* (Springer, 1987).
44. T. G. Wright, EigTool software; www.cs.ox.ac.uk/projects/pseudospectra/eigtool/ (2002).
45. G. H. Golub, C. F. van Loan, *Matrix Computations* (Johns Hopkins Univ. Press, ed. 3, 1996).
46. V. I. Arnold, *Ordinary Differential Equations* (Springer, 2006).
47. C. Chicone, *Ordinary Differential Equations with Applications* (Springer-Verlag, 1999).
48. J. Almunia, G. Basterretxea, J. Aristegui, R. E. Ulanowicz, Benthic-pelagic switching in a coastal subtropical lagoon. *Estuar. Coast. Shelf Sci.* **49**, 363–384 (1999).
49. Pajek datasets; <http://vlado.fmf.uni-lj.si/pub/networks/> (2018).
50. R. E. Ulanowicz, *Growth and Development: Ecosystems Phenomenology* (Springer-Verlag, 1986).
51. M. E. Monaco, R. E. Ulanowicz, Comparative ecosystem trophic structure of three U.S. mid-Atlantic estuaries. *Mar. Ecol. Prog. Ser.* **161**, 239–254 (1997).
52. J. Hagy, “Eutrophication, hypoxia and trophic transfer efficiency in Chesapeake Bay,” thesis, University of Maryland (2002).
53. D. Baird, R. E. Ulanowicz, The seasonal dynamics of the Chesapeake Bay ecosystem. *Ecol. Monogr.* **59**, 329–364 (1989).
54. D. Baird, J. Luczkovich, R. Christian, Assessment of spatial and temporal variability in ecosystem attributes of the St Marks National Wildlife refuge, Apalachee Bay, Florida. *Estuar. Coast. Shelf Sci.* **47**, 329–349 (1998).

55. R. E. Ulanowicz, J. J. Heymans, M. S. Egnatovich, "Annual report to the United States Geological Service Biological Resources Division" (ref. no. [UMCES] CBL 00-0176, Chesapeake Biological Laboratory, University of Maryland, 2000).
56. J. Kunegis, The KONECT project; <http://konect.cc/> (2017).
57. N. D. Martinez, J. J. Magnuson, T. Kratz, M. Sierszen, Artifacts or attributes? Effects of resolution on the Little Rock Lake food web. *Ecol. Monogr.* **61**, 367–392 (1991).
58. M. Kaiser, C. C. Hilgetag, Nonoptimal component placement, but short processing paths, due to long-distance projections in neural systems. *PLOS Comput. Biol.* **2**, e95 (2006).
59. S. S. Shen-Orr, R. Milo, S. Mangan, U. Alon, Network motifs in the transcriptional regulation network of *Escherichia coli*. *Nat. Genet.* **31**, 64–68 (2002).
60. J. Duch, A. Arenas, Community detection in complex networks using extremal optimization. *Phys. Rev. E* **72**, 027104 (2005).
61. R. M. Ewing, P. Chu, F. Elisma, H. Li, P. Taylor, S. Climie, L. McBroom-Cerajewski, M. D. Robinson, L. O'Connor, M. Li, R. Taylor, M. Dharsee, Y. Ho, A. Heilbut, L. Moore, S. Zhang, O. Ornatsky, Y. V. Bukhman, M. Ethier, Y. Sheng, J. Vasilescu, M. Abu-Farha, J.-P. Lambert, H. S. Duetel, I. I. Stewart, B. Kuehl, K. Hogue, K. Colwill, K. Gladwish, B. Muskat, R. Kinach, S.-L. Adams, M. F. Moran, G. B. Morin, T. Topaloglou, D. Figeys, Large-scale mapping of human protein–protein interactions by mass spectrometry. *Mol. Sys. Biol.* **3**, 89 (2007).
62. J.-F. Rual, K. Venkatesan, T. Hao, T. Hirozane-Kishikawa, A. Dricot, N. Li, G. F. Berriz, F. D. Gibbons, M. Dreze, N. Ayivi-Guedehoussou, Towards a proteome-scale map of the human protein-protein interaction network. *Nature* **437**, 1173–1178 (2005).
63. Federal Aviation Administration, Flight delay information - Air traffic control system command center; www.fly.faa.gov/ (2017).
64. T. Opsahl, Why anchorage is not (that) important: Binary ties and sample selection; <http://wp.me/poFcy-Vw> (2011).
65. G. Storch, P. Dell'Olmo, M. Gentili, 9th DIMACS implementation challenge - Shortest paths; www.dis.uniroma1.it/challenge9 (2006).
66. R. W. Eash, K. S. Chon, Y. J. Lee, D. E. Boyce, Equilibrium traffic assignment on an aggregated highway network for sketch planning. *Transp. Res. Record* **994**, 30–37 (1983).
67. D. E. Boyce, K. S. Chon, M. E. Ferris, Y. J. Lee, K.-T. Lin, R. W. Eash, Implementation and evaluation of combined models of urban travel and location on a sketch planning network. *Chicago Area Transp. Stud.* xii + 169 (1985).
68. T. Opsahl, P. Panzarasa, Clustering in weighted networks. *Soc. Netw.* **31**, 155–163 (2009).
69. J. Leskovec, D. Huttenlocher, J. Kleinberg, Signed network in social media, in *Proceedings of the SIGCHI Conference on Human Factors in Computing Systems* (Association for Computing Machinery, 2010), pp. 1361–1370.
70. J. Leskovec, D. Huttenlocher, J. Kleinberg, Predicting positive and negative links in social networks, in *Proceedings of the 19th International Conference on World Wide Web* (Association for Computing Machinery, 2010), pp. 641–650.
71. J. Leskovec, A. Krevl, SNAP datasets: Stanford large network dataset collection; <http://snap.stanford.edu/data> (2014).
72. B. Klimt, Y. Yang, The Enron corpus: A new dataset for email classification research, in *Proceedings of the 15th European Conference on Machine Learning* (Springer, 2004), pp. 217–226.
73. J. Leskovec, J. Kleinberg, C. Faloutsos, Graph evolution: Densification and shrinking diameters. *ACM Trans. Knowl. Discov. Data* **1**, 2 (2007).
74. M. Ley, The DBLP computer science bibliography: Evolution, research issues, perspective, in *International Symposium on String Processing and Information Retrieval* (Springer, 2002), pp. 1–10.
75. J. S. Coleman, Introduction to mathematical sociology, in *London Free Press Glencoe* (CAB International, 1964).
76. L. C. Freeman, C. M. Webster, D. M. Kirke, Exploring social structure using dynamic three-dimensional color images. *Soc. Netw.* **20**, 109–118 (1998).
77. J. Coleman, E. Katz, H. Menzel, The diffusion of an innovation among physicians. *Sociometry* **20**, 253–270 (1957).
78. L. A. Adamic, N. Glance, The political blogosphere and the 2004 U.S. election: Divided they blog, in *Proceedings of the 3rd International Workshop on Link Discovery* (Association for Computing Machinery, 2005), pp. 36–43.
79. M. D. Choudhury, H. Sundaram, A. John, D. D. Seligmann, Social synchrony: Predicting mimicry of user actions in online social media, in *Proceedings of the International Conference on Computational Science and Engineering* (Association for Computing Machinery, 2009), pp. 151–158.
80. M. Richardson, R. Agrawal, P. Domingos, Trust management for the semantic web, in *International Semantic Web Conference* (Springer, 2003), pp. 351–368.

Acknowledgments: Gratitude goes to D. Fanelli and P. K. Maini for useful discussions.

Funding: The work of M.A. and T.C. presents research results of the Belgian Network DYSCO, funded by the Interuniversity Attraction Poles Programme, initiated by the Belgian State, Science Policy Office. The work of M.A. was also supported by an FRS-FNRS Postdoctoral Fellowship. **Author contributions:** M.A. and T.C. designed the study, conducted the formal analysis, and analyzed the data. All authors organized and wrote the manuscript. **Competing interests:** The authors declare that they have no competing interests. **Data and materials availability:** All data needed to evaluate the conclusions in the paper are present in the paper and/or the Supplementary Materials. Additional data related to this paper may be requested from the authors.

Submitted 30 July 2018

Accepted 14 November 2018

Published 12 December 2018

10.1126/sciadv.aau9403

Citation: M. Asllani, R. Lambiotte, T. Carletti, Structure and dynamical behavior of non-normal networks. *Sci. Adv.* **4**, eaau9403 (2018).

Structure and dynamical behavior of non-normal networks

Malbor Asllani, Renaud Lambiotte and Timoteo Carletti

Sci Adv 4 (12), eaau9403.
DOI: 10.1126/sciadv.aau9403

ARTICLE TOOLS

<http://advances.sciencemag.org/content/4/12/eaau9403>

SUPPLEMENTARY MATERIALS

<http://advances.sciencemag.org/content/suppl/2018/12/10/4.12.eaau9403.DC1>

REFERENCES

This article cites 50 articles, 12 of which you can access for free
<http://advances.sciencemag.org/content/4/12/eaau9403#BIBL>

PERMISSIONS

<http://www.sciencemag.org/help/reprints-and-permissions>

Use of this article is subject to the [Terms of Service](#)

Science Advances (ISSN 2375-2548) is published by the American Association for the Advancement of Science, 1200 New York Avenue NW, Washington, DC 20005. 2017 © The Authors, some rights reserved; exclusive licensee American Association for the Advancement of Science. No claim to original U.S. Government Works. The title *Science Advances* is a registered trademark of AAAS.